Available online at www.sciencedirect.com
SCIENCE DIRECT®
Journal of Solid State Chemistry 177 (2004) 1425–1430
JOURNAL OF SOLID STATE CHEMISTRY
http://elsevier.com/locate/jssc

Synthesis and characterization of nanocrystalline tin oxide by sol–gel method

Jianrong Zhang and Lian Gao*

Shanghai Institute of Ceramics, Chinese Academy of Sciences, State Key Laboratory of High Performance Ceramics and Superfine Microstructure, Shanghai 200050, People's Republic of China

Received 17 September 2003; received in revised form 17 November 2003; accepted 23 November 2003

Abstract

Nanocrystalline SnO_2 particles have been synthesized by a sol–gel method from the very simple starting material granulated tin. The synthesis leads a sol–gel process when citric acid is introduced in the solution obtained by dissolving granulated tin in HNO_3. Citric acid has a great effect on stabilizing the precursor solution, and slows down the hydrolysis and condensation processes. The obtained SnO_2 particles range from 2.8 to 5.1 nm in size and 289–143 $m^2 g^{-1}$ in specific surface area when the gel is heat treated at different temperatures. The particles show a lattice expansion with the reduction in particle size. With the absence of citric acid, the precursor hydrolyzes and condenses in an uncontrollable manner and the obtained SnO_2 nanocrystallites are comparatively larger in size and broader in size distribution. The nanocrystallites have been characterized by means of TG-DSC, FT-IR, XRD, BET and TEM.

Keywords: Tin oxide; Nanocrystallite; Wet chemical method; Sol–gel

1. Introduction

Tin oxide (SnO_2), cassiterite structure, is a typical wide band gap n-type semiconductor (3.8 eV) [1] and one of the most widely used semiconductor oxides due to its chemical and mechanical stabilities. It can be used as transparent electrodes for solar cells, liquid crystal displays; catalysts for methanol conversion and CO/O_2, CO/NO reaction in the control of noxious emissions; antistatic coatings and gas sensors; anodes for lithium-ion batteries, transistors, catalyst supports; nano and ultrafiltration membranes and anticorrosion coatings [2–14]. When doped with certain elements, such as In, Sb, and F, SnO_2 exhibits greatly increased electric conductivity and become transparent for visible light and reflective for IR radiation. They are members of the transparent conductive oxides (TCOs), which have become the focus of intensified study as possible components in solid-state optoelectronic devices [1,6,12,15–17]. Among the various applications, the most important use of SnO_2 is for gas sensors. The sensing properties of SnO_2 sensors (sensitivity, selectivity and reproducibility) depend on several factors, mainly crystallite size and specific surface area. For example, the sensitivity begins to increase sharply as crystallite size (D) decreases below a critical value (6 nm), which is equal to twice the thickness of the Schottky barrier penetrating into the tin oxide grains. The whole crystallite is depleted of electrons, as a result, the sensitivity of the element to a reducing gas would change with D. Reactions between oxygen species and reducing gases to be detected can be improved by increasing the sensing surface area. Consequently, the use of nanoparticles will allow obtaining better responses of these solid-state gas sensors [3,4,13]. It is well known that the sintering and densification of SnO_2 is very difficult [18]; particles in nanoscale size and less agglomerated are expected to be sintered at lower temperature [19]. In the field of lithium-ion battery, very fine tin oxide particles are needed to obtain high capacity [11]. So it is of great importance to synthesize nanoscale tin oxide particles.

Tin oxide nanoparticles were prepared by many different wet chemical methods, such as precipitation [9–11,13,14,20], hydrothermal [3,10], solvothermal [21], sol–gel [2,10,16,22], gel-combustion [23], spray pyrolysis [24], polymerized complex (PC) [25] and amorphous

*Corresponding author. Fax: +86-21-52413122.
E-mail address: liangaoc@online.sh.cn (L. Gao).

0022-4596/$ - see front matter © 2003 Elsevier Inc. All rights reserved.
doi:10.1016/j.jssc.2003.11.024

citrate [26] method. Starting from tin chlorides ($SnCl_4$ or $SnCl_2$) is generally preferred because they are easy to perform and the cost is very low, but the chlorine ions are very difficult to remove and the residual chlorine ions often affect the surface and electrical properties, introducing a random n-type doping in the material [27], modifying the sensitivity of sensors [28], causing agglomeration among particles [29] and leading to higher sintering temperatures [19]. Tin alkoxides $Sn(OR)_n$ are better alternatives to synthesize SnO_2 nanoparticles free from chlorides, but the metal alkoxides are comparatively more expensive and cannot be used on a large scale. Another drawback of metal alkoxides is that they are particularly moisture sensitive and have to be processed under a dry and inert atmosphere, and the resulting OXO-polymers that constitute the sols and gels are generally polydispersed in size and composition [2,7,10,22,24]. Angelina et al. [16] synthesized F-doped tin oxide nanoparticles from tin (IV) complexes, $(CH_3COCHCOCH_3)_2SnF(Otert\text{-}Am)$ and $(CF_3COCHCOCH_3)_2Sn(otert\text{-}Am)_2$; the synthesis procedures of the precursors and the nanoparticle are especially complex. The gel-combustion method needs a large amount of organics and produces large volume of gases such as NO_x and CO_2 during the combustion reaction. Nicolas et al. [13] synthesized high surface area SnO_2 nanoparticles by direct oxidation of Sn in HNO_3, but the synthesis procedure is hard to control and the particle-specific surface area decreased sharply to only about $24\,m^2\,g^{-1}$ when heated at 600°C.

In this paper, we report the synthesis of tin oxide nanocrystallites by novel wet chemical methods from granulated tin. The starting materials are very cheap and the synthesis procedures are simple, and the obtained SnO_2 particles are in nanometer scale and monodispersed with very large surface areas. This should be a better choice instead of the sol–gel method from tin alkoxides. The particles have been characterized by means of TG-DSC, FT-IR, XRD, BET and TEM.

2. Experimental procedure

2.1. Synthesis of SnO_2 nanocrystallites by the sol–gel method

$8\,mol\,L^{-1}$ HNO_3 was carefully added to a mixture of 3 g of granulated tin and 10 g of citric acid in a flask until a clear solution was obtained. Aqueous ammonia (25%) was added dropwise into the solution with stirring until a pH value of 8 was reached. The obtained solution was refluxed at 100°C for 2 h, During refluxing the solution slowly turned into a turbid colloidal solution. After cooling down, the sol was collected from the solution by centrifugation and washed several times with water and ethanol. After drying at 100°C for 5 h in air, the obtained gel powder was ground in a mortar, and finally calcined in a muffle furnace at 300°C, 400°C, 500°C for 2 h.

2.2. Synthesis of SnO_2 nanocrystallites by the direct precipitation method

The synthesis procedure was similar to the sol–gel method except that no citric acid was added. Precipitate was obtained as soon as aqueous ammonia was added into the solution. When the pH value of the solution reached 8, another 2 h of reaction was needed. The precipitate was washed with water and ethanol, dried at 100°C for 5 h, and finally heated at different temperatures for 2 h.

2.3. Characterization

Simultaneous thermogravimetry and differential scanning calorimetry (TG-DSC) were carried out with a Netasch STA 449 analyser. Experiments were carried out under N_2 at a heating rate of $10°C\,min^{-1}$.

Fourier-transformed infrared spectra (FT-IR) were recorded on Nicolet Magna 550 spectrometer (32 scans at a resolution of $4\,cm^{-1}$). The particles were pelleted with dried KBr and analyzed in transmission mode.

The crystallites of the particles were characterized by powder X-ray diffraction (XRD) with a Rigaku Model D/max rb 2550v diffractometer using Cu$K\alpha$ radiation ($\lambda = 1.5406$ Å) at 40 kV and 60 mA, by scanning at $2°\,(2\theta)\,min^{-1}$. The lattice parameters were obtained by a least-squares refinement [30]. The average crystallite size (D) of the SnO_2 particles was calculated from the half-height line broadening by applying the Scherrer formula and assuming Gaussian profiles for experimental and instrumental broadening [1].

The specific surface area of the nanocrystallites was measured with a Micromeritics ASAP 2010 analyzer using the multipoint Brunauer, Emmett and Teller (BET) adsorption method. The average grain size (d) of the SnO_2 particles was calculated from the formula $d = 6/\rho A$, where ρ is the theoretical density of the material and A is the specific surface area of the powder [10,22,23].

The morphology of the nanocrystallites was observed by transmission electron microscopy (TEM) with JEM-200CX TEM.

3. Results and discussion

3.1. Synthesis of SnO_2 nanocrystallite with citric acid as a complexing agent

Two heavy weight losses are observed in Fig. 1, the TG and DSC curves of the dried gel. The first weight

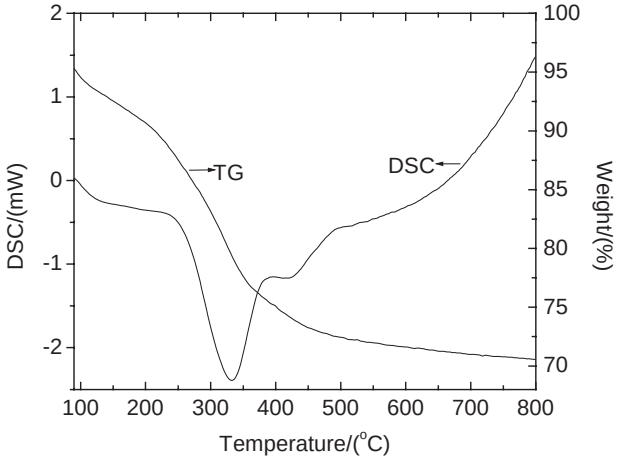

Fig. 1. TG-DSC curves of the dried gel synthesized by the sol–gel method.

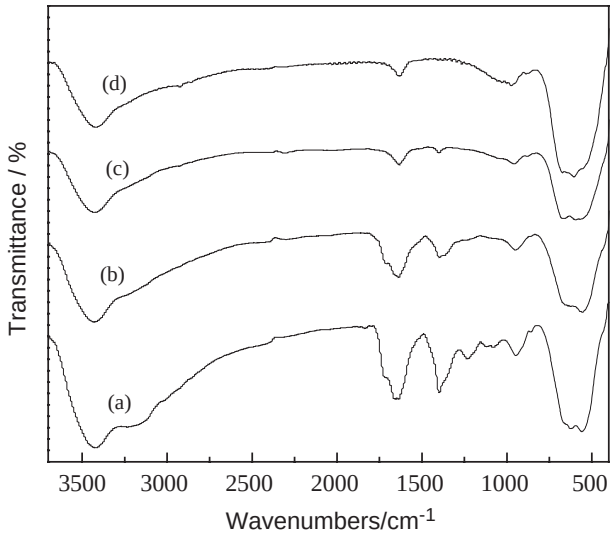

Fig. 2. FT-IR spectra of SnO_2 gel treated at different temperatures. (a) 100°C; (b) 200°C; (c) 400°C; (d) 600°C.

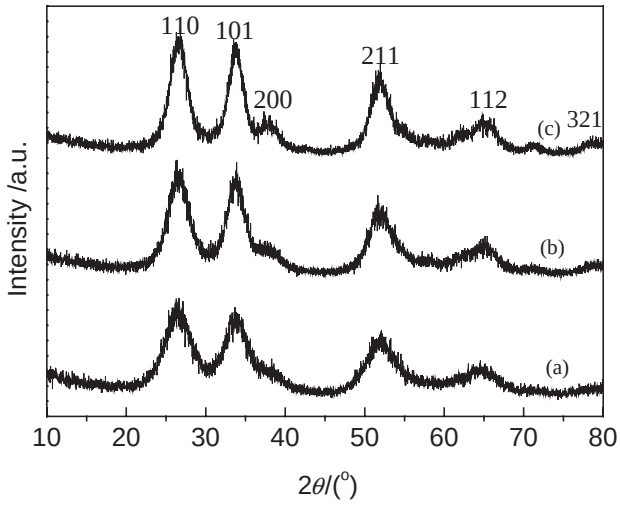

Fig. 3. XRD patterns of the SnO_2 nanocrystallites synthesized by the sol–gel method treated at different temperatures. (a) 300°C; (b) 400°C; (c) 500°C.

loss (6.8%, RT to 140°C) with an endothermic feature likely corresponds to the evaporation of free water and residual free EtOH. The second weight loss (22.4% ca. 500°C) with a heavy exothermal feature is related to the decomposition of citrate groups and NO_3^- ions, and the condensation of Sn-OH surface groups. Above 500°C, the weight remains constant and has no endo- or exothermal character.

Fig. 2 shows the FT-IR spectra of the dried gel after heat treatment at different temperatures. In Fig. 2(a) the strong vibration extending from 3500 to 2500 cm^{-1} indicates the presence of hydrogen bonds involved in O–H oscillators [9,16,33], arising from adsorbed water and Sn-OH groups. In solid citrate the carboxyl groups are ionized, so the peak at 1662 cm^{-1} can be assigned to COO^- group vibration of the citrate complex [31,32], A shoulder peak at 1710 cm^{-1} probably corresponds to the COOR groups, caused by the dimer of free citric acid. The peak at 1398 cm^{-1} can be ascribed to the bending vibration of NO_3^- ions occluded in the gel [32]. The peaks between 1232 and 900 cm^{-1} are attributed to the vibration of hydroxyl-tin bonds [6]. The vibration at 560 cm^{-1} is related to the terminal oxygen vibration of Sn-OH and the peak at 660–600 cm^{-1} is attributable to the OXO bridge functional groups (OSnO) [9,13,16], which reveals that the tin citrate complex gel has been partly transformed to tin oxide. As the heat treatment temperature increases, the absorption intensity of the COO^- group decreases due to the decomposition of the citrate complex, and the peak at 560 cm^{-1} also decreases steadily, and finally disappears at >400°C, which indicates that the tin citrate complex transforms to tin oxide completely.

Fig. 3 shows the XRD patterns of the powders obtained at different temperatures; the peak positions in each sample agree well with the reflections of bulk SnO_2 (cassiterite). The width of the reflections is considerably broadened, indicating a small crystalline domain size. The broadenings decrease with the increase of heat treatment temperatures, suggesting the growth of the SnO_2 crystallites. The average crystallite sizes (D) determined from (110) crystalline plane are listed in Table 1. It can be seen that all the particles are in nanometer scale and grow slowly with the increase of heat treatment temperature. The particle size is about 5.1 nm at 773 K, which is the smallest to the authors' knowledge. The lattice parameters of the SnO_2 crystallites determined by the least-squares refinement are also listed in Table 1. All the samples exhibit larger cell volumes than that of bulk SnO_2 ($V = 71.55$ Å^3, JCPDS 41-1445) and show a linear decrease with the increase of heat treatment temperature, in other words, with the

Table 1
Crystallite sizes, specific surface areas, average grain sizes and unit-cell parameters of the SnO_2 nanocrystallites synthesized by the sol–gel method treated at different temperatures

Temperature (°C)	Crystallite size (nm)	Surface area ($m^2 g^{-1}$)	Grain size (nm)	Unit-cell parameters		
				a (Å)	c (Å)	V (Å^3)
300	2.8	289.1	2.9	4.778	3.170	72.369
400	4.0	209.9	4.1	4.756	3.186	72.065
500	5.1	143.1	5.6	4.750	3.184	71.840

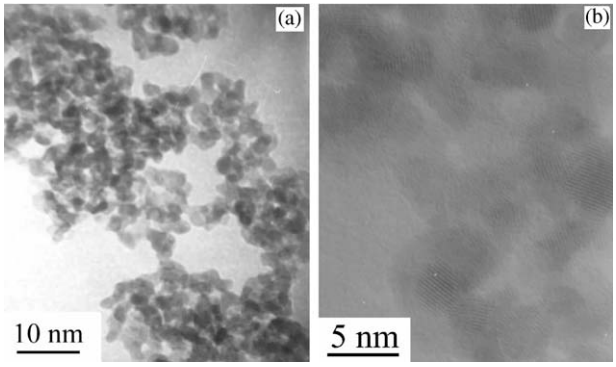

Fig. 4. TEM image (a) and HREM image (b) of the SnO_2 nanocrystallites synthesized by the sol–gel method treated at different temperatures. (a) 300°C; (b) 500°C.

increase of the crystallite size. These results agree well with the conclusion that oxide nanoparticles exhibit a lattice expansion with the reduction in particle size [33].

Specific surface areas of the SnO_2 nanocrystallites determined by the BET method are listed in Table 1. The data are much larger than the SnO_2 synthesized by the precipitation, citrate amorphous and hydrothermal methods [8,10,20,23,26]. The specific surface areas decrease steadily with the increase of heating temperatures due to the growth and packing of the nanocrystallites. The calculated average grain sizes (d) coincide well with those from the broadening of XRD peaks at lower temperatures, while at higher temperatures, the average grain size is larger than the crystallite size, indicating a low degree of agglomeration.

Fig. 4 shows the TEM images of the SnO_2 nanocrystallites synthesized by the sol–gel method. In Fig. 4(a) the crystallites obtained at 300°C for 2 h are shown. The particles fall within the range of 2–3 nm, the size distribution is very narrow and the nanocrystallites are monodispersed. The residual C element from the citric acid that had not been combusted yet is shown in the EDS. In Fig. 4(b) the HREM image of the nanocrystallites calcined at 500°C for 2 h is shown. Most crystallites are about 5 nm with clear lattice strings. The connected crystallites form a random network, in which there are many clearly nano-sized holes; this structure is called a "nano-sponge structure." The particles show a small degree of agglomeration, in agreement with the results previously obtained. No residual C is element shown in the EDS, which is consistent with the TG-DSC revealed.

3.2. Synthesis of SnO_2 nanocrystallites by the direct precipitation method

Fig. 5 shows the XRD patterns of the powders synthesized by the direct precipitation method. All peaks show the same cassiterite structure and are widely broadening, revealing that nanoscale SnO_2 particles can also be synthesized by this method. But the widths of the peaks are comparatively narrower than the crystallites synthesized by the sol–gel method at the same temperatures. Table 2 lists the average crystallite sizes calculated by the Scherrer formula from the (110) plane.

Specific surface areas and corresponding average grain sizes are also shown in Table 2. Compared with the sol–gel-synthesized SnO_2, the specific surface areas are smaller and the average grain sizes are larger. The comparisons of the average crystallite sizes and the

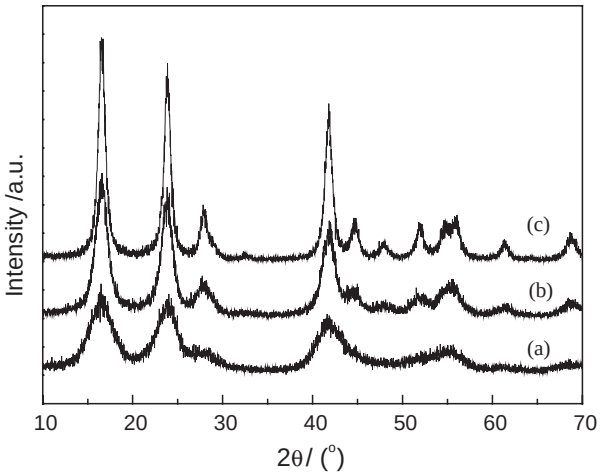

Fig. 5. XRD patterns of the SnO_2 nanocrystallites synthesized by the direct precipitation method treated at different temperatures. (a) 300°C; (b) 400°C; (c) 500°C.

Table 2
Crystallite sizes, specific surface areas and average grain sizes of the SnO_2 nanocrystallites synthesized by the direct precipitation method treated at different temperatures

Temperature (°C)	Crystallite size (nm)	Surface area ($m^2 g^{-1}$)	Grain size (nm)
300	5.1	161.1	5.3
400	8.4	75.0	11.4
500	15.2	32.2	26.6

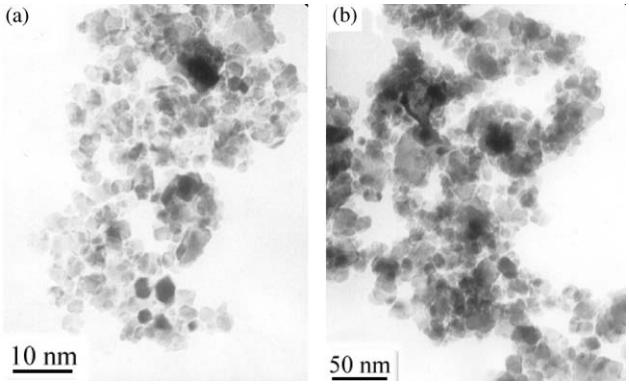

Fig. 6. TEM images of the SnO_2 nanocrystallites synthesized by the direct precipitation method treated at different temperatures. (a) 300°C; (b) 500°C.

corresponding average grain sizes reveal that the degree of agglomeration increases sharply with the heat treatment temperatures. The TEM images in Figs. 6(a) and (b) also reveal this tendency and a broad size distribution ranging from 12 to 35 nm and an average size of 20 nm are observed in the 500°C heat-treated nanocrystallites.

3.3. *Effect of citric acid in the synthesis of SnO_2 nanocrystallites*

The mechanism of synthesizing SnO_2 nanocrystallites with the addition of citric acid can be called a "citric acid-based sol–gel method."

It is well known that the sol–gel method is a versatile solution technique used to obtain ultrafine, homogenous powders of a variety of glass and ceramic materials at low temperature and in short time through the growth of metal oxo-polymers in a solvent. The chemistry involved in the sol–gel process is based on the inorganic polymerization of molecular precursors. The sol–gel process involves hydrolysis and condensation, which are generally fast and need to be inhibited to avoid precipitation and allow sol or gel formation [2,24]. Complexation is a popular method of modifying the original precursors, and carboxylic acid or β-diketones are the most frequently used modifying ligands, which slow down the pace of hydrolysis and condensation [16,22,24].

Citric acid is the widely used complexing agent [24,30,31,34,35]. As previously pointed out, citric acid (H_3L) is a weak triprotic acid and dissociates in a stepwise manner in solution depending upon the solution pH; only when pH value of the solution is above 6.4 [34], the species L becomes the dominant one. The complexation reactions between metal ions and citric acid are also highly dependent upon the solution pH and cannot occur in a very strong acidic solution, so we adjusted the pH value of the precursor solution to about 8. We found that during the continuous addition of NH_4H_2O the solution turned turbid and again clear, and very stable when the pH value was about 8, while the solution without the addition of citric acid as complexing agent was unstable and hydrolyzed in a few minutes, which evidenced that the complexing reaction occurred. Another advantage of pH value being adjusted to about 8 was that the isoelectrical point of the SnO_2 powder lies at a pH of 2.5–3.7 [12,15], the Zeta potential values are negative and constant for $pH > 5$, so the degree of agglomeration can be greatly decreased at the settled pH value. Strong acidic conditions enhanced the hydrogen bonding among the protonated nanocrystallites, leading to a high degree of agglomeration, while in higher pH value solutions, the coordinated water molecules should suppress the agglomeration among the freshly formed nanocrystallites.

As the chelated tin has 6-fold coordination instead of 4 in inorganic starting materials [2,22], its reactivity is greatly lowered. The general formula is $M(OOR)_n$, (M refers to Sn), and when the solution was refluxed at 373 K, the solution changed into sol slowly and the controlled sol–gel process can be described as follows [32]:

Hydrolysis:

$$M(OOR)_n + xH_2O \rightarrow M(OOR)_{n-x}(OH)_x + xRCOOH.$$

Condensation:

$$2M(OOR)_{n-x}(OH)_x \rightarrow [(OH)_{x-1}(OOR)_{n-x}M]_2O + H_2O.$$

When the gel was heat treated at different temperatures, SnO_2 nanocrystallites having very small size and very high specific surface areas were obtained. But in the direct precipitation method, hydrolysis of the precursor was very fast, nucleation and growth were completed within seconds, the SnO_2 particles formed were unstable and a white suspension was immediately formed due to the precipitation of large aggregates. The same phenomena have been observed in other solutions containing simple inorganic nitrates and did not allow to attain a good homogeneity at atomic scale. The obtained SnO_2 nanocrystallites were comparatively larger and had lower specific surface areas, but when compared with SnO_2 nanoparticles prepared from tin chlorides, the prepared SnO_2 nanocrystallites have a larger specific surface area, which may be ascribed to the absence of chlorine ions [29].

Upon heating at higher temperatures, the specific surface areas of the sol–gel-obtained SnO_2 nanocrystallites decreased, especially at above 500°C, which can be explained as follows. In the citric acid-based sol–gel method, the complexing ligands may also act as a surface-protecting agent, protecting the newly

transformed nanocrystallites from contacting each other and the agglomeration was avoided (just as seen in the TEM image). With the removal of the complexing agents at higher temperatures, this protecting effect also disappeared and the surface areas decreased. For the same reason, the specific surface areas of the direct precipitated SnO_2 nanocrystallites decreased more sharply.

When considering the size distribution of the nanocrystallites, Yin et al. [35] found that the addition of citric acid in the hydrothermal synthesis of TiO_2 nanocrystallites led to a very narrow size distribution of the particles. They explained that citric acid coordinated to titanium ions in $TiCl_4$ aqueous solution, making the nucleation complete at the early stage of the hydrothermal process and inhibiting the crystal growth. We suggest that in the sol–gel process the coordination between citric acid and Sn ions also makes the nucleation process complete at the early stage of the sol–gel process, leading to a narrow size distribution of the SnO_2 nanocrystallites. In the absence of citric acid (the direct precipitation method), the nucleation process is comparatively slow and leads to a solid-state epitaxial crystal growth mechanism, which results in a very broad size distribution of the SnO_2 nanocrystallites.

4. Conclusions

Tin oxide nanocrystallites are successfully synthesized by the wet chemical methods from the starting material granulated tin. The added citric acid coordinates with tin ions and slows down the hydrolysis and condensation of the precursor, inducing nucleation at the early stage of the sol–gel process. Monodispersed SnO_2 nanocrystallites ranging from 2.8 to 5.1 nm in size and 289–143 $m^2 g^{-1}$ in specific surface areas are obtained when the gel is given heat-treatment at different temperatures. However, in the absence of citric acid, the hydrolysis and condensation are very fast, and comparatively larger and heavier agglomerated SnO_2 nanocrystallites are formed. Generally, the starting material is low cost and the synthesis processes are very simple, which should be a good choice instead of the sol–gel method from metal alkoxides to synthesize metal oxide nanocrystallites. This method can also be utilized to synthesize many other doped tin oxide nanocrystallites.

References

[1] J. Rockenberger, U. Felde, M. Tischer, L. Troger, M. Haase, H. Weller, J. Chem. Phys. 112 (2000) 4296.
[2] S. Monredon, A. Cellot, F. Ribot, C. Sanchez, L. Armelao, L. Gueneau, L. Delattre, J. Mater. Chem. 12 (2002) 2396.
[3] N.-S. Baik, G. Sakai, N. Miura, N. Yamazoe, J. Am. Ceram. Soc. 83 (2000) 2983.
[4] E.S. Rembeza, O. Richard, J.V. Landuyt, Mater. Res. Bull. 34 (1999) 1527.
[5] T. Mori, S. Hoshino, A. Neramittagapong, J. Kubo, Y. Morikawa, Chem. Lett. 29 (2002) 390.
[6] Y.J. Lin, C.J. Wu, Surf. Coat. Technol. 88 (1996) 239.
[7] C. Nozaki, K. Tabata, E. Suzuki, J. Solids State Chem. 154 (2000) 579.
[8] S. Loridant, J. Phys. Chem. B 106 (2002) 13273.
[9] L. Abello, B. Bochu, A. Gaskov, S. Koudryavtseva, G. Lucazeau, M. Roumyantseva, J. Solid State Chem. 135 (1998) 78.
[10] M. Ristic, M. Ivanda, S. Popovic, S. Music, J. Non-Crystal. Solids 303 (2002) 270.
[11] A.C. Bose, D. Kalpana, P. Thangadurai, S. Ramasamy, J. Power sources 107 (2002) 138.
[12] C. Gobbert, M.A. Aegerter, D. Burgard, R. Nass, H. Schmidt, J. Mater. Chem. 9 (1999) 253.
[13] N. Sergent, P. Gelin, L.P. Camby, H. Praliaud, G. Thomas, Sensors Actuators B 84 (2002) 176.
[14] G.H. Philip, C.L. Nicholas, D. Wayne, B. Craig, A. Wan, Chem. Mater. 11 (1999) 896.
[15] M.J. Van bommmel, W.A. Groen, H.A.M. Vanhal, W.C. Keur, T.N.M. Bernards, J. Mater. Sci. 34 (1999) 4803.
[16] A. Gamard, O. Babaot, B. Jousseaucne, M.C. Rascle, T. Toupance, G. Campet, Chem. Mater. 12 (2000) 3419.
[17] T.T. Emons, J.Q. Li, L.F. Nazar, J. Am. Chem. Soc. 124 (2002) 8516.
[18] G.E.S. Brito, S.H. Pulcinellli, C.V. Santilli, N. Barelli, J. Mater. Sci. Lett. 12 (1993) 992.
[19] O. Vasykiv, Y. Sakka, J. Am. Ceram. Soc. 84 (2001) 2489.
[20] J.A. Toledo-Antonio, R. Gutierrez-Baez, P.J. Sebastian, A. Vazquez, J. Solid State Chem. 174 (2003) 241.
[21] Z.X. Deng, C. Wang, Y.D. Li, J. Am. Ceram. Soc. 85 (2002) 2837.
[22] L. Broussous, C.V. Santilli, S.H. Pulcinelli, A.F. Craievich, J. Phys. Chem. B 106 (2002) 2855.
[23] L. Fraigi, D.G. Lamas, N.E.W. Reca, Nanostruct. Mater. 11 (1999) 311.
[24] M. Kakihana, J. Sol–Gel Sci. Technol. 6 (1996) 7.
[25] E.R. Leite, A.P. Maciel, I.T. Weber, P.N.L. Filho, E. Longo, C.O.P. Santos, A.V.C. Andrade, C.A. Pakoscimas, Y. Manietle, W.H. Schreiner, Adv. Mater. 14 (2002) 905.
[26] M. Bhagwat, P. Shah, V. Ramaswamy, Mater. Lett. 57 (2003) 1604.
[27] J.S. Pena, T. Brousse, L. Sanchez, J. Morales, D.M. Schleich, J. Power Sources 97–98 (2001) 232.
[28] N. Sergent, P. Gelin, L. Perier-Camby, H. Praliaud, G. Thomas, Sensors Actuators B 84 (2002) 176.
[29] A. Roosen, H. Hausener, Adv. Ceram. Mater. 3 (1988) 131.
[30] Y.W. Song, Y. Ma, H. Xiong, Y.Q. Jia, M.L. Liu, M.Z. Jin, Mater. Chem. Phys. 78 (2003) 660.
[31] J.D. Tsay, T.T. Fang, J. Am. Ceram. Soc. 82 (1999) 1409.
[32] W.-X. Kuang, Y.-N. Fan, K-W. Yao, Y. Chen, J. Solid State Chem. 140 (1998) 354.
[33] P. Ayyub, V.R. Palkar, S. Chattopadhyay, M. Multani, Phys. Rev. B 51 (1995) 6135.
[34] J.-H. Choy, Y.-S. Han, J. Mater. Chem. 7 (1997) 1815.
[35] H.B. Yin, Y. Wada, T. Kitamura, T. Sumida, Y. Hasegawa, S. Yanagida, J. Mater. Chem. 12 (2002) 378.